9950-1148
DOE/JPL-956615-85/05

LASER-ASSISTED SOLAR CELL METALLIZATION PROCESSING

A. Rohatgi, S. Gupta, P. G. McMullin
and P. A. Palaschak

Quarterly Report for the Period December 1984 to February 1985

Jet Propulsion Laboratory
Contract No. 956615

April 4, 1985

Westinghouse R&D Center
1310 Beulah Road
Pittsburgh, Pennsylvania 15235

LASER-ASSISTED SOLAR CELL METALLIZATION PROCESSING

A. Rohatgi, S. Gupta, P. G. McMullin
and P. A. Palaschak

Quarterly Report for the Period December 1984
to February 1985

Jet Propulsion Laboratory
Contract No. 956615

April 4, 1985

Westinghouse R&D Center
1310 Beulah Road
Pittsburgh, Pennsylvania 15235

TABLE OF CONTENTS

LIST OF FIGURES

1. SUMMARY

In this contract, laser-assisted processing techniques for producing high-quality solar cell metallization patterns are being investigated, developed, and characterized. The tasks comprising these investigations are outlined in the milestone chart shown in Figure 1.

During this period a new batch of solar cells was processed using the laser decomposition of spun-on silver neodecanoate to metallize cells. Decomposition of silver neodecanoate was carried out at different laser powers on different cells on a given wafer to determine whether this would have any effect on cell performance. A one watt laser power gave an electroplated linewidth of 50 μm, while at 8 watts the line width was 90 μm. Unfortunately, these cells could not be finished and tested because the grid lines came off from this particular wafer during the photoresist/mismatch step which is used to define the cell area. This experiment is being repeated.

The rest of the batch, which was written with laser powers of 5-8 watts, gave excellent results with cell efficiencies in the range of 14-16%. Dark I-V measurements showed that in most cases series resistance was less than 0.5 ohm-cm^2 and shunt resistance was greater than 10^3 kΩ-cm^2. There was no noticeable difference in cell efficiencies at different laser powers in the range of 5-8 watts. This was consistent with the Dektak examination, which showed no variation in linewidth with the different laser powers. Linewidth in all cases was approximately 100 μm, indicating that the beam was not focused directly on the wafer surface. Careful focusing experiments are now being performed in order to achieve finer linewidths. We have obtained a lens with shorter focal length, f = 50 mm, as opposed to the old lens with f = 80 mm. This should provide much tighter focusing and finer lines.

JPL CONTRACT 956615, MODIFICATION 2

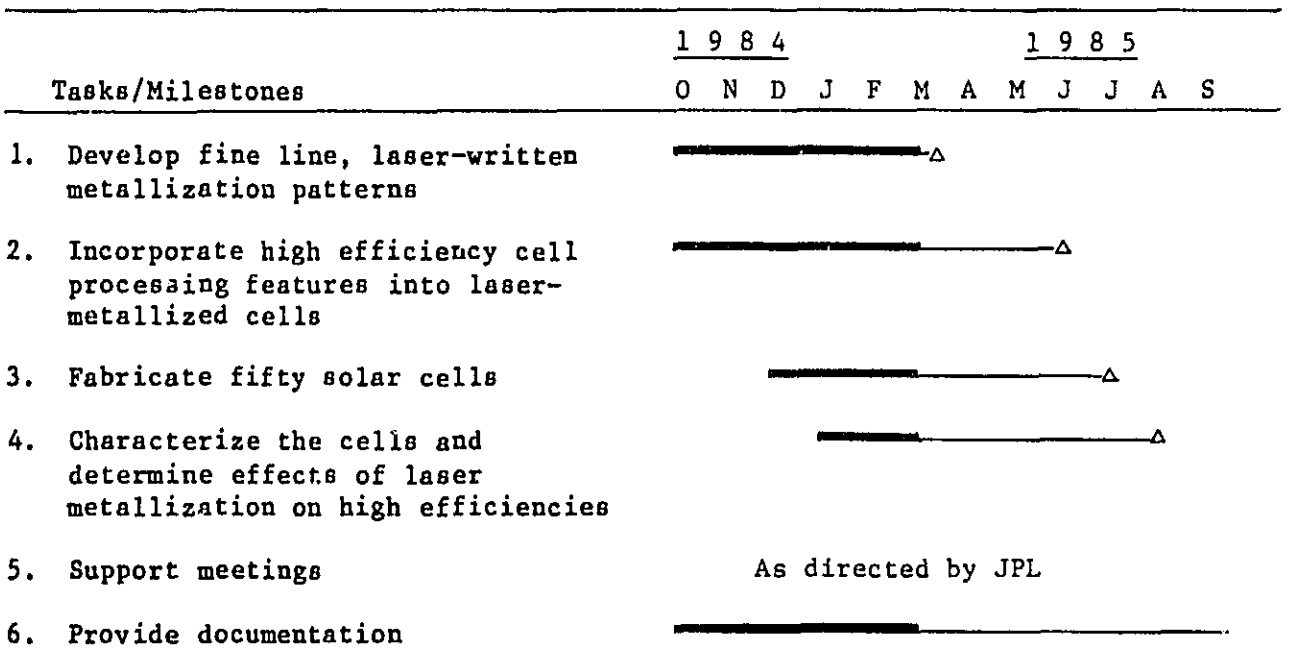

Figure 1. Milestone Chart.

In an attempt to achieve even higher efficiencies, we have initiated a solar cell run with low-resistivity (0.25 Ω-cm) Wacker float-zone silicon, which has to date given us ≥ 18% efficient cells with surface passivation and double-layer AR coating using the conventional photoresist processing and metallization. Solar cells will now be fabricated on low-resistivity three-inch diameter wafers instead of the 4 Ω-cm two-inch diameter float-zone silicon used in the past.

The challenge now is to incorporate surface passivation in the laser-metallized cell processing sequence, which does not allow photolithography for grid delineation. So far two approaches have been taken: firstly, to grow ~30 Å nitride for passivation, which may either allow tunneling of carriers from silicon to the grid lines or breakdown under the grid line during laser processing; secondly, to grow 100 Å thick passivating oxide and try to zap it by laser processing. Initial results on the latter approach look promising, although more work is required to determine whether this method is reproducible.

2. TECHNICAL PROGRESS

2.1 Laser-Metallized Cells on 4 ohm-cm Float-Zone Silicon

A new batch of solar cells was processed using the laser decomposition of spun-on silver neodecanoate to metallize the cells. Decomposition of the silver neodecanoate was carried out at different laser powers to determine whether this would have any effect on cell efficiency. Consistently high efficiencies, ranging from 14% to nearly 16%, were obtained for the AR-coated cells.

Silver neodecanoate was spun onto several Ti-Pd-coated, diffused, two-inch silicon wafers. Twelve comb patterns were written on each wafer using a focused argon-ion laser, at laser powers of 5 W, 6 W, 7 W, and 8 W, and subsequently electroplated. The titanium and palladium coatings were etched, mesas were defined and etched, double-layer AR coatings were evaporated, and the cells were characterized.

Certain problems were encountered during cell processing. There was some wafer staining during the palladium and titanium etching process steps. This staining occurred when the wafer was replaced in the aqua regia etch for palladium after the titanium etch failed to remove all the metal evenly. This uneven etching may have been caused by a thin film of silver adhering to certain regions of the Ti-Pd-coated wafer during electroplating. In the future, after electroplating, the wafers will be placed in a diluted silver etch prior to the other metal etches.

Another problem arose when the double-layer AR coating was evaporated before mesa definition. The photoresist did not adhere well to the AR coating, and the mesa etch undercut the metallization patterns, ruining the wafers that were laser metallized at 8 W. The process steps were reversed for the remaining wafers, the mesa etch

being performed before evaporation of the AR coating, resulting in high-quality cells.

Previous studies have shown that linewidths are dependent on laser power. This experiment, using a range of laser powers, was designed to determine the effect of laser power on cell efficiency, higher efficiencies being expected with narrower linewidths. However, Dektak profiles of the laser-written lines, both before and after electroplating, showed that the lines were all approximately 100 μm wide, regardless of laser power. This clearly indicated that the beam was not focused on the wafer surface. The lighted I-V data for the cells metallized at 7 W, 6 W, and 5 W are presented in Tables 1, 2, and 3, respectively, and the corresponding dark I-V data are presented in Tables 4, 5, and 6, respectively. As expected, because of the similar linewidths measured, the cells metallized at the different laser powers are seen to have similar efficiencies, ranging from 14% to nearly 16%. These are excellent values, especially considering that there is significant cell shadowing due to the wide lines. The laser metallization process, therefore, consistently yields high-quality cells.

The results of the above experiment indicated that the laser beam was not focused onto the wafer surface. To determine the position of the focus accurately, lines were written on a test wafer coated with silver neodecanoate for a range of lens positions.

At focus, comb metallization patterns were written on a Ti-Pd-coated, diffused wafer which had silver neodecanoate spun on. Laser powers ranging from 8 W to 1 W were used. Nomarski photomicrographs of the lines were taken before and after the silver neodecanoate was rinsed off, and after electroplating for 40 minutes up to a thickness of 1 μm. The linewidths for the various powers, as measured from these photographs, are presented in Table 7. It may be seen that the lines do not broaden appreciably upon electroplating. A surprising result was that the comb pattern written at 1 W, which appeared to consist primarily of carbon deposits with little or no silver, plated up as uniformly as the

Table 1

Lighted I-V Data For 4 ohm-cm Solar Cells Laser Metallized At 7 W

Cell I.D.	Short-Circuit Current(mA)	Open-Circuit Voltage(V)	Fill Factor	Efficiency (%)
Q6-1	33.0	0.584	0.779	15.0
Q6-2	33.1	0.582	0.784	15.1
Q6-3	33.5	0.581	0.781	15.2
Q6-4	32.7	0.580	0.781	14.8
NB55-1	32.4	0.579	0.789	14.8
NB55-2	30.2	0.578	0.791	13.8
NB55-3	30.7	0.579	0.787	14.0
NB55-4	32.0	0.575	0.785	14.5
NB55-5	32.9	0.580	0.761	14.5
NB55-6	30.6	0.577	0.788	13.9
NB55-7	32.5	0.579	0.762	14.3
NB55-8	32.4	0.577	0.767	14.3
NB55-11	33.0	0.573	0.783	14.8
NB55-12	33.1	0.570	0.787	14.9

Table 2

Lighted I-V Data For 4 ohm-cm Solar Cells Laser Metallized At 6 W

Cell I.D.	Short-Circuit Current(mA)	Open-Circuit Voltage(V)	Fill Factor	Efficiency %
Q7-1	33.0	0.566	0.789	14.7
Q7-2	33.2	0.567	0.790	14.9
Q7-3	33.6	0.565	0.783	14.9
Q7-4	33.6	0.566	0.775	14.8
Q7-5	33.2	0.563	0.780	14.6
Q7-6	33.3	0.561	0.786	14.7
Q7-7	33.1	0.561	0.788	14.6
Q7-8	33.0	0.565	0.763	14.2
Q7-9	32.0	0.562	0.787	14.1
Q7-10	32.0	0.563	0.789	14.1
Q7-11	33.0	0.567	0.784	14.6
Q7-12	33.0	0.566	0.784	14.5
NB60-1	32.9	0.581	0.774	14.8
NB60-2	32.4	0.584	0.795	15.0
NB60-3	33.2	0.585	0.792	15.4
NB60-4	33.3	0.582	0.788	15.3
NB60-5	34.2	0.586	0.755	15.1
NB60-7	31.1	0.576	0.791	14.2
NB60-8	32.0	0.576	0.781	14.4
NB60-11	31.6	0.573	0.789	14.3
NB60-12	33.3	0.579	0.790	15.2

Table 3

Lighted I-V Data For 4 ohm-cm Solar Cells Laser Metallized At 5 W

Cell I.D.	Short-Circuit Current(mA)	Open-Circuit Voltage(V)	Fill Factor	Efficiency (%)
Q10-1	34.2	0.593	0.740	15.0
Q10-2	34.1	0.589	0.780	15.7
Q10-3	34.2	0.587	0.770	15.5
Q10-4	33.5	0.575	0.756	14.6
Q10-5	34.1	0.584	0.693	13.8
Q10-6	33.8	0.580	0.782	15.3
Q10-7	34.4	0.585	0.783	15.8

Table 4

Dark I-V Data For ohm-cm Solar Cells Laser Metallized At 7 W

Cell I.D.	Normalized Series Resistance (Ω-cm^2)	Normalized Shunt Resistance (kΩ-cm^2)	J_{01}(A/cm^2)	J_{02}(A/cm^2)
Q6-1	0.3	$> 10^3$	2.9×10^{-12}	6.5×10^{-9}
Q6-2	0.3	$> 10^3$	4.0×10^{-12}	3.4×10^{-8}
Q6-3	0.3	909.6	3.8×10^{-12}	7.7×10^{-9}
Q6-4	0.3	$> 10^3$	2.7×10^{-12}	3.9×10^{-8}
NB55-1	0.4	$> 10^3$	3.4×10^{-12}	8.6×10^{-9}
NB55-2	0.4	0	3.4×10^{-12}	1.1×10^{-8}
NB55-3	0.5	$> 10^3$	3.5×10^{-12}	2.0×10^{-8}
NB55-4	0.6	500.3	4.0×10^{-12}	2.3×10^{-8}
NB55-5	0.7	3.7	3.3×10^{-12}	3.0×10^{-5}
NB55-6	1.4	51.6	6.3×10^{-12}	9.7×10^{-7}
NB55-7	0.7	$> 10^3$	2.2×10^{-12}	4.5×10^{-8}
NB55-8	0.7	417.0	2.8×10^{-12}	5.1×10^{-8}
NB55-11	0.7	$> 10^3$	4.5×10^{-12}	9.7×10^{-9}
NB55-12	0.7	$> 10^3$	5.1×10^{-12}	1.1×10^{-8}

Table 5

Dark I-V Data For 4 ohm-cm Solar Cells Laser Metallized At 6 W

Cell I.D.	Normalized Series Resistance (Ω-cm^2)	Normalized Shunt Resistance (kΩ-cm^2)	J_{01}(A/cm^2)	J_{02}(A/cm^2)
Q7-1	0.5	$> 10^3$	5.8×10^{-12}	1.4×10^{-8}
Q7-2	0.5	$> 10^3$	6.0×10^{-12}	2.0×10^{-8}
Q7-3	0.5	$> 10^3$	6.6×10^{-12}	4.5×10^{-8}
Q7-4	0.6	$> 10^3$	6.2×10^{-12}	3.6×10^{-8}
Q7-5	0.6	33.1	6.8×10^{-12}	7.5×10^{-8}
Q7-6	0.7	$> 10^3$	7.8×10^{-12}	6.8×10^{-8}
Q7-7	0.7	$> 10^3$	7.2×10^{-12}	1.8×10^{-8}
Q7-8	0.6	$> 10^3$	6.3×10^{-12}	3.3×10^{-8}
Q7-9	0.7	0	6.9×10^{-12}	2.5×10^{-8}
Q7-10	0.7	$> 10^3$	6.4×10^{-12}	1.3×10^{-8}
Q7-11	0.7	$> 10^3$	5.0×10^{-12}	5.0×10^{-8}
Q7-12	0.7	24.0	5.7×10^{-12}	3.3×10^{-7}
NB60-1	0.2	122.0	3.6×10^{-12}	2.1×10^{-7}
NB60-2	0.2	476.?	3.3×10^{-12}	2.8×10^{-8}
NB60-3	0.3	909.2	2.8×10^{-12}	9.3×10^{-9}
NB60-4	0.3	39.2	3.6×10^{-12}	1.7×10^{-7}
NB60-5	0.4	1.2	3.1×10^{-12}	8.6×10^{-5}
NB60-7	0.5	31.9	4.0×10^{-12}	3.9×10^{-8}
NB60-8	0.4	2.5	4.4×10^{-12}	2.4×10^{-5}
NB60-11	0.5	$> 10^3$	4.7×10^{-12}	3.6×10^{-8}
NB60-12	0.5	79.4	4.0×10^{-12}	6.7×10^{-8}

Table 6

Dark I-V Data For 4 ohm-cm Solar Cells Laser Metallized At 5 W

Cell I.D.	Normalized Series Resistance (Ω-cm^2)	Normalized Shunt Resistance (kΩ-cm^2)	J_{01}(A/cm^2)	J_{02}(A/cm^2)
Q10-1	0.5	137.0	2.8×10^{-12}	3.2×10^{-8}
Q10-2	0.3	$> 10^3$	2.8×10^{-12}	1.2×10^{-9}
Q10-3	0.4	$> 10^3$	2.7×10^{-12}	5.3×10^{-8}
Q10-4	0.7	277.8	4.8×10^{-12}	2.1×10^{-8}
Q10-5	0.9	$> 10^3$	3.5×10^{-12}	8.7×10^{-9}
Q10-6	0.5	$> 10^3$	2.7×10^{-12}	5.1×10^{-10}
Q10-7	0.5	$> 10^3$	3.2×10^{-12}	6.5×10^{-9}

Table 7

Linewidths As A Function of Laser Power Before and After Electroplating

Laser Power (W)	Linewidths (μm)		
	Before Film Rinse	After Film Rinse	After 40 min. Electroplating
8	80	85	90
6	80	80	85
4	70	70	75
2	60	65	70
1	60	50	50

rest of the patterns. These patterns can now be used to determine the effect of linewidth on cell efficiency. Unfortunately, the grid lines peeled off during the photoresist/mesa etch step and the cells could not be completed for testing. It should be noted that this problem is not related to the lower laser powers used because even the pattern which was written with 8 W peeled off. We plan to repeat this experiment.

A shorter focal length lens, f = 50 mm, has been obtained and a suitable lens holder has been machined. This should provide much tighter focusing than the present lens, which has focal length of 80 mm, resulting in finer lines.

2.2 Cell Fabrication On Low-Resistivity Float-Zone Wacker Silicon

A solar cell run has been initiated with three-inch diameter, p-type, (100), 0.25 Ω-cm float-zone material from Wacker Siltronix. This material has the potential of giving higher efficiency cells compared to the 4 Ω-cm float-zone silicon used in this program in the past. Switching to this new material is expected to show that laser metallization is suitable for fabricating even higher than 16-16.5% efficient cells, which have already been demonstrated on 4 Ω-cm float-zone silicon wafers.[1] This first run, expected for completion in two to three weeks, will also have laser-written comb patterns using silver neodecanoate film with laser powers varying from 1 to 8 watts.

2.3 Front-Surface Passivation in Laser-Metallized Cells

Surface recombination is a dominant loss mechanism in solar cells. Several investigators[2-5] have shown that surface passivation by a 100 Å thick thermal oxide can produce a 1-2% (absolute) improvement in cell performance. Improved cell efficiency is usually associated with an increase in V_{oc} and J_{sc}.

In conventional surface-passivated cells, contact windows are opened by photolithography and subsequently the contact grid lines are defined by a lift-off process followed by plating. Since the major

objective of laser-metallized cell processing is to by-pass photolithography and define the grid lines by laser writing, the problem is whether to grow a very thin tunnel oxide for passivation, or somehow zap the 100 Å passivating oxide under the grid lines while laser writing. Otherwise the oxide impedance will degrade cell performance.

MOS experiments have been initiated for the purpose of finding a solution to the above problem without having to go through expensive and time-consuming cell fabrication. These experiments involve either growth of 110 Å oxide by thermal oxidation at 900°C, or deposition of 40 Å nitride by the low-pressure CVD technique. After the dielectric growth, 30 mil diameter, 10,000 Å thick Al dots were evaporated to form the ohmic contact. MOS dots were then sintered at 450°C/30 min in H_2 to reduce the interface state density, although during this heat treatment the Ti-Pd dots turned brownish. At present the reason for this is not known. It should be noted that Ti-Pd contacts are being used for the MOS capacitors, which is consistent with the process sequence of laser-metallization of cells.

As expected, a typical MOS C-V curve was observed (Figure 2) prior to laser treatment. High-frequency capacitance-voltage measurements were performed at 1 MHz frequency. The typical C-V curve indicates that an insulator is present between the contact metal and silicon. This was also verified by the I-V measurements on the curve tracer (Figure 3), which showed no appreciable current flow through the dielectric. However, after laser scanning the MOS dots with 8 watt laser power, the dielectric began to conduct and the MOS capacitor broke down. Although these results were anticipated, the resistance measured after the breakdown was still ~100 ohms. It is not clear if this is due to the probe making contact with Pd or because of the partial dielectric breakdown. Figure 4 shows the traces of the laser scan over the MOS dot, which was done with the 110 Å oxide; more experiments are in progress with the oxide and nitride passivating layers. In this experiment MOS capacitors were sintered at 450°C/30 min in H_2 prior to laser scanning. Selection of the dielectric and the laser power for

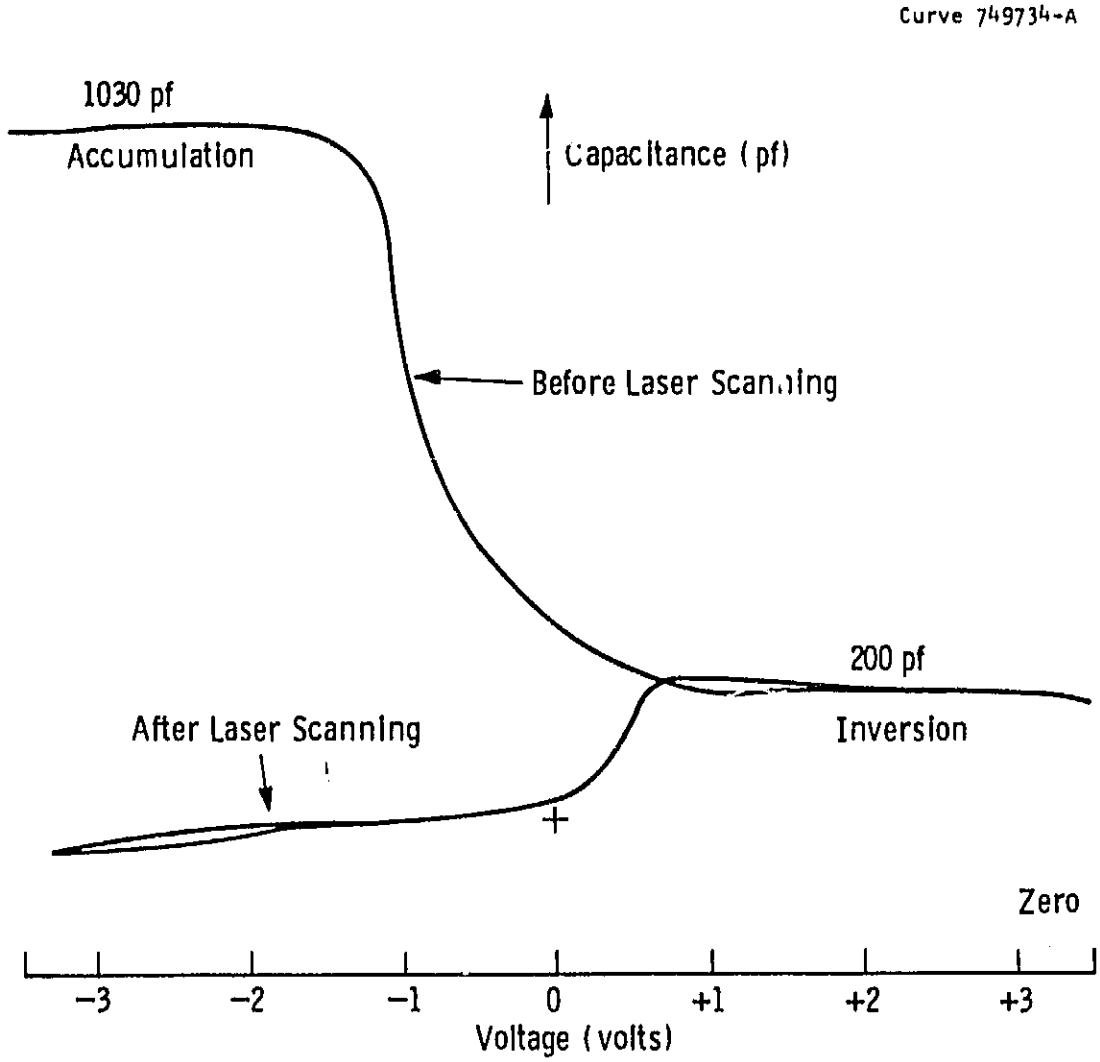

Figure 2. High-frequency capacitance-voltage curves before and after laser scanning. A sharp drop in the accumulation capacitance at negative voltage indicates dielectric breakdown (Dot #1).

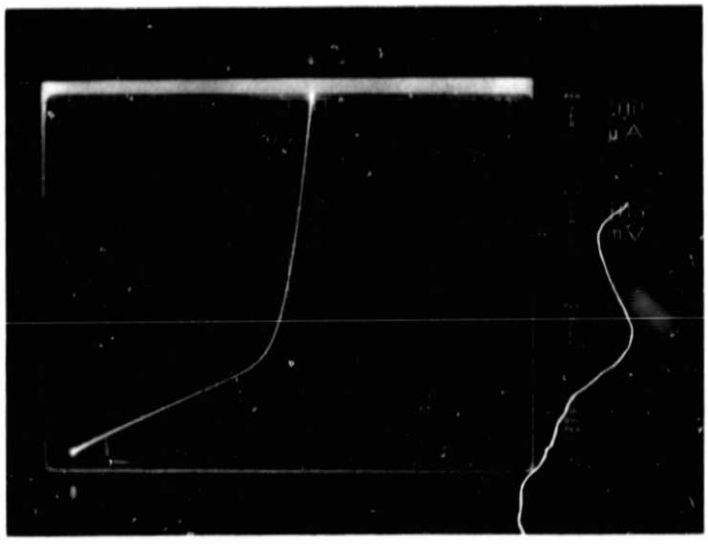

Figure 3. I-V curve of the MOS capacitor after laser scanning; insulator becomes a conductor after laser scanning (Dot #1).

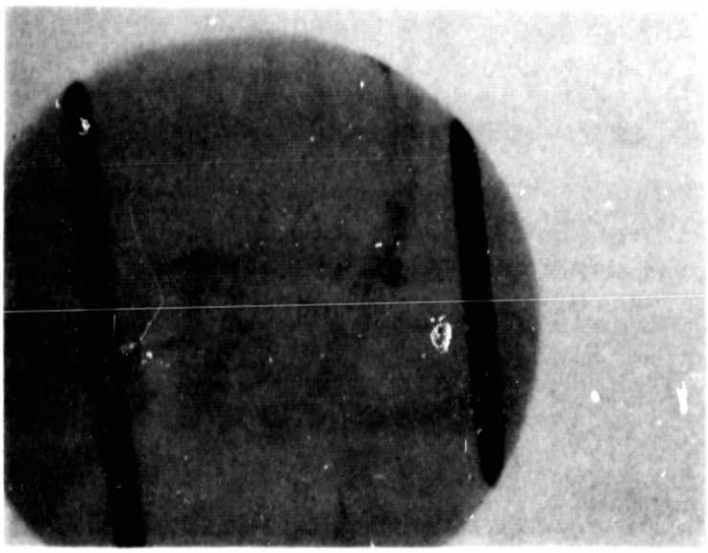

Figure 4. Traces of laser scans on the 30-mil diameter MOS Dot #1; dark lines delineate the traces.

writing the actual grid lines for the passivated laser-metallized solar cells will be based on the success of these experiments. Solar cells with ≥ 18% efficiency have been fabricated on this 0.25 ohm-cm float-zone silicon using oxide passivation and evaporated double-layer AR coating by the conventional process. If the surface passivation can be successfully implemented in the laser-metallized cells, then laser-metallized cell efficiencies in excess of 18% should be obtained, provided laser processing produces no adverse effects.

3. PROGRAM STATUS

3.1 Present Status

The current milestone chart for this program was shown as Figure 1. Accomplishments during this three-month period include:

- Grid patterns have been written with laser powers varying from 1 to 8 W.
- Cells with 14-16% efficiencies have been fabricated on 4 ohm-cm float-zone silicon by laser decomposition of silver neodecanoate.
- A solar cell run was initiated using low-resistivity (0.25 ohm-cm) float-zone silicon.
- Passivating oxide and nitride have been grown on silicon wafers followed by an attempt to zap the dielectric with laser scanning.

3.2 Future Activity

Plans are to define narrow grid lines using the new lens, complete a solar cell run with low-resistivity wafers, and continue the effort to incorporate surface passivation in laser-metallized cells.

4. ACKNOWLEDGMENTS

The authors wish to thank J. B. McNally and F. S. Youngk for assistance in cell processing; S. Karako for cell testing and MOS-CV8IV measurements; and G. S. Law for manuscript editing and preparation.

5. REFERENCES

1. S. Dutta, P. G. McMullin, P. A. Palaschak, and P. Rai-Choudhury, Annual Report on Laser-Assisted Solar Cell Metallization Processing, JPL Contract No. 956615 (September 1984).

2. A. Rohatgi and P. Rai-Choudhury, IEEE Trans. on Electron Devices, ED-31, No. 5, p. 661 (1984).

3. M. B. Spitzer, S. P. Tobin, and C. J. Kearney, IEEE Trans. on Electron Devices, ED-31, No. 5, p. 546 (1984).

4. M. A. Green et al., Proc. 17th IEEE Photovoltaic Specialists Conf., p. 386 (1984).

5. A. Rohatgi et al., Proc. 17th IEEE Photovoltaic Specialists Conf., p. 409 (1984).